

A sum-over-state scheme of analysis of hyperpolarizabilities and its application to spiroconjugated molecular system

Nabamita Panja · Tapan K. Ghanty ·

Prasanta K. Nandi

Received: 31 August 2009 / Accepted: 4 November 2009 / Published online: 25 November 2009
© Springer-Verlag 2009

Abstract The static first and second hyperpolarizabilities of a number of spiomolecules with varying degree of polarity have been calculated at the HF and MP2 level using the 6-31+G* basis set and the B3LYP/6-31+G* optimized geometry. The variation of mean second hyperpolarizability in these molecular systems has been explained in terms of the ground state dipole moment, mean linear polarizability and second-order polarizability. A number of relationships among these quantities have been derived in the framework of the sum-over-state scheme and the generalized Thomas–Kuhn sum rule. The spiroconjugation results in the significant increase of the mean polarizability. The appreciable enhancement of first hyperpolarizability due to the spiroconjugation between two dipolar monomer units has been accounted for the rather significant increase of the mean polarizability tensor and the ground state dipole moment. The relatively larger value of the average second hyperpolarizability of the spiroconjugated molecules compared to that of the corresponding monomers arises from the rather significant increase of the nonaxial component γ_{xyy} . The replacement of spirocarbon by spirosilicon results in the enhancement of the cubic polarizability manifold. The donor–acceptor substituted spirocompounds are predicted to be the superior third-order nonlinear optical (NLO) phores. The nature of π -conjugation in the monomer units around the spirocenter shows a strong modulation of the NLO properties of

spirocompounds. The influence of electron correlation on the NLO properties at the MP2 level has been found to be rather significant.

Keywords Spirolinked molecules · Nonlinear polarizabilities · Sum-over-state (SOS) scheme · Electron correlation

1 Introduction

Nonlinear optics (NLO) is currently an active area of research. There have been many attempts to find compounds with large hyperpolarizabilities. The compounds considered for this purpose are mostly organic charge transfer chromophores which consist of electron donor and electron-withdrawing groups attached at the two ends of a π -conjugative system. Organic molecular systems with extended π -delocalization [1–7] have been investigated both theoretically and experimentally because of their relatively greater thermal stability, low cost, ease of fabrication and integration into devices and possessing many attractive NLO characteristics, i.e., ultrafast response times, lower dielectric constants, large susceptibility, ease of modification, etc. While organic crystals and polymers are envisioned for applications, the theoretical study of isolated molecular species should provide many useful informations, which may be important in refining the fundamental understanding of the NLO properties of materials. Thus, quantum chemical calculations and analysis may guide the synthetic efforts aimed at optimizing the molecular hyperpolarizabilities.

Spiroconjugated molecular systems draw a special kind of attention because of their exceptionally larger NLO properties [8–15] compared to the corresponding monomers

N. Panja · P. K. Nandi (✉)
Department of Chemistry, Bengal Engineering and Science University, Shibpur, Howrah 711103, India
e-mail: nandi_pk@yahoo.co.in

T. K. Ghanty
Theoretical Chemistry Section, Chemistry Group,
Bhabha Atomic Research Centre, Mumbai 400085, India

although the respective lowest-energy electronic transition frequency shows rather small shift. The recent theoretical investigations of the photo-physical and optical properties of spirolinked oligofluorene [16] and spirosilabifluorene derivatives [17] showed good optical transparency and the strong two-photon absorptions. The enhancement of first hyperpolarizability of spirocompounds has been explained based on the orbital interaction through the spirolinkage.

Most of the earlier investigations [11–15] of the optical properties of the spirolinked compounds considered the first hyperpolarizability although attempts [8, 9] were also made to calculate the second hyperpolarizability of such molecular species. There have been significant progresses in the task of designing potential NLO materials since the well documented structure–property correlation studies [18, 19] of hyperpolarizabilities of intramolecular charge transfer chromophores. For the dipolar molecules the two state model and for the nondipolar noncentrosymmetric molecules the three state model consisting of the truncated standard sum-over-state (SOS) expressions [20, 21] have been used widely to interpret the origin of first hyperpolarizability. Likewise, the truncated SOS expression has been used to explain the relative variation of second hyperpolarizability in different class of molecular systems. The theoretically calculated value of NLO properties, however, depends largely on the level of computation employed. Besides other factors the electron correlation effects are very much important while comparing the theoretically calculated value of hyperpolarizabilities with that obtained from experimental measurements. However, the general trend of NLO properties in connection to the structure–property correlations can be predicted satisfactorily at a given level of calculation [22].

Although the recent computational facility may be useful for calculating the electric response properties of moderately larger molecules with a desirable degree of accuracy by employing the appropriate quantum chemical methods using large basis sets, still it seems to be rather difficult task to predict the accurate higher-order polarizabilities for rather larger molecular systems of interest. Therefore, the general relationships between polarizabilities of different-order (α , β and γ) might be useful to theoreticians as well as experimentalists to rationalize the results obtained and to find the important parameters to adjust for optimum efficiency. A number of investigations [18, 19, 23–26] in this direction may be mentioned where the qualitative dependence between the third-order polarizability (γ) and the linear polarizability (α) has been noted. The experimentally measurable reorientational contribution to the second hyperpolarizability is directly related to the polarizability anisotropy ($\Delta\alpha$) of a molecule [27]. A number of useful relationships between the axial components of hyperpolarizabilities, polarizability and the ground state electric

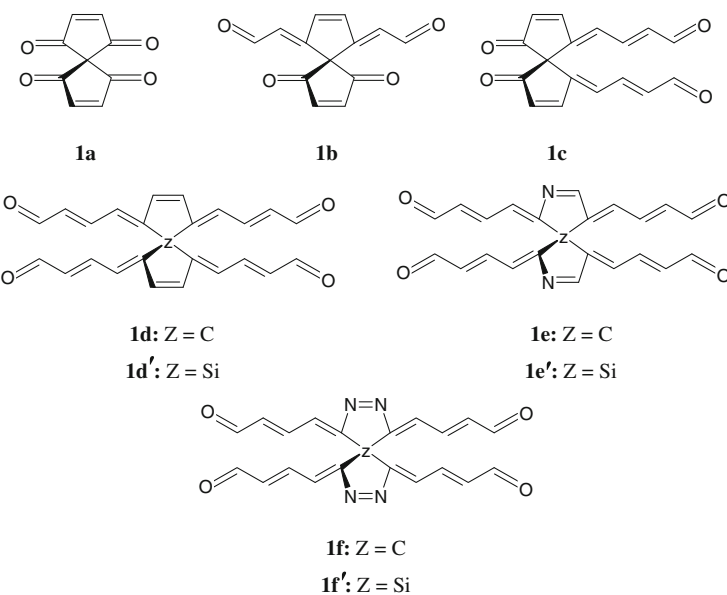
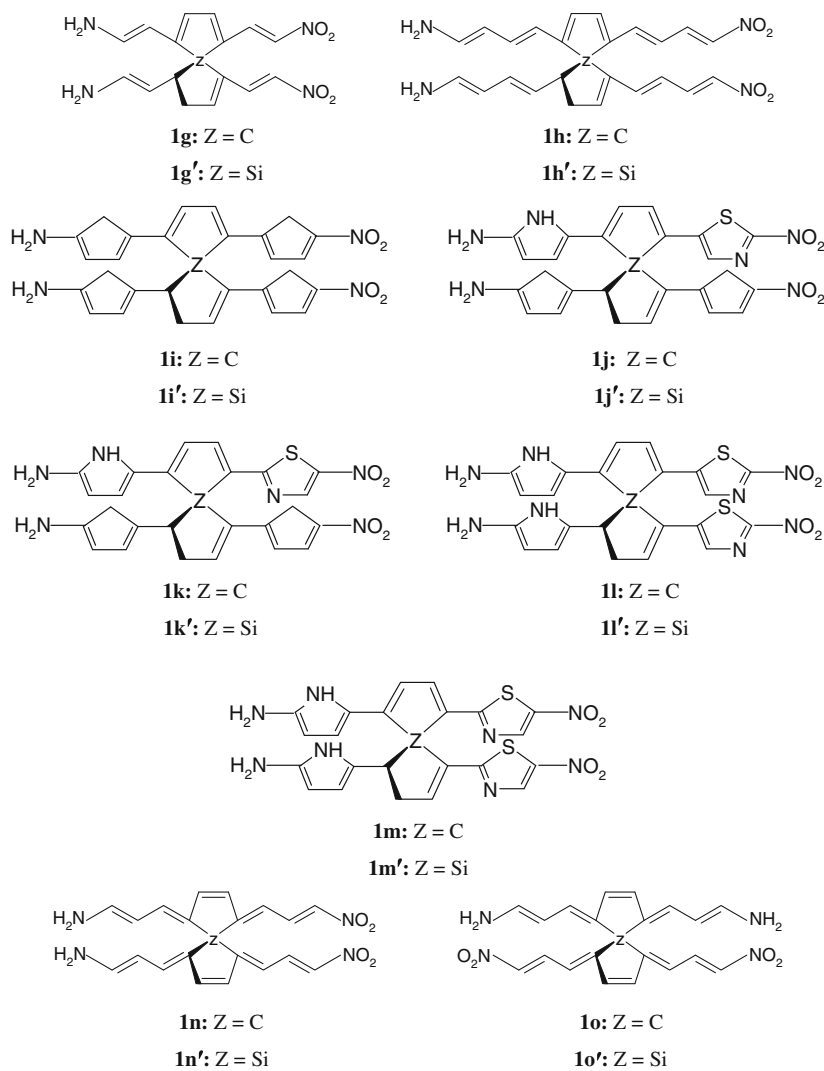
moments have recently been derived by us [28, 29] and employed them to rationalize the variation of NLO responses for different kind of molecular systems investigated. In the present investigation, we have intended to derive relationships between the experimentally measurable quantities, such as mean second hyperpolarizability ($\langle\gamma\rangle$), vector part of first hyperpolarizability (β_{vec}), mean polarizability ($\bar{\alpha}$) and ground state dipole moment (μ_g) in the framework of the standard SOS expressions [20, 21] and the generalized Thomas–Kuhn (TK) sum rule [30, 31]. The necessary task is to simplify the terms involving both the axial and nonaxial components of hyperpolarizabilities in the SOS expression. Second, we used these relationships to explain the variation of the axial and nonaxial components of hyperpolarizabilities obtained for the chosen spirocompounds (Scheme 1) so that meaningful full structure–property correlations can be predicted.

The investigated spirolinked molecules consist of two identical or different structural units which are connected through a tetrahedral carbon atom called a spirocenter. The spiroconjugative effect on the hyperpolarizabilities arising from the C and Si spirocenter has also been addressed. The molecules chosen in the present work are model chromophores and have not been studied so far. We have considered molecules **1a–1d'** with the polyene chains disposed symmetrically or unsymmetrically around the spirocenter, and molecules **1e–1f'** having the electronegative nitrogen atom in the conjugative paths with an objective to find the effect of these structural modifications on the NLO properties. Since the extension of π -conjugation and the presence of electron-donating and electron-withdrawing groups at the ends of a charge transfer conduit generally lead to the enhancement of the optical nonlinearity, a number of donor–acceptor (DA) substituted spirocompounds **1g–1o'** have also been selected to find whether similar such effect can be found for these molecular systems and to which extent. Some representative monomer molecules denoted by **1d_m**, **1d'_m**; **1e_m**, **1e'_m** and **1n_m**, **1n'_m** (not shown in Scheme 1) corresponding to molecules **1d**, **1d'**; **1e**, **1e'** and **1n**, **1n'** (Scheme 1) have also been considered for the sake of comparison of their NLO properties with those of the dimers.

2 Computational methods

2.1 Electronic structure and properties

The ground state equilibrium geometry of the chosen molecules (Scheme 1) has been fully optimized at the B3LYP level with 6-31+G* basis set. The static linear and nonlinear polarizabilities of each molecule were computed at the HF/6-31+G*/B3LYP/6-31+G* and MP2/6-31+G//

Scheme 1**Donor-Acceptor Systems**

B3LYP/6-31+G* levels using the finite field (FF) scheme. The polarizability components were calculated from the field-perturbed energy of a molecule. All calculations were done by using the GAMESS program [32]. The mean static linear polarizability ($\bar{\alpha}$) has been defined as one-third of the trace of linear polarizability tensor.

$$\bar{\alpha} = (\alpha_{xx} + \alpha_{yy} + \alpha_{zz})/3 \quad (1)$$

The vector part of second-order polarizability (β) which has generally been reported in the EFISH experiment is given by,

$$\beta_{\text{vec}} = \frac{\mu_x \beta_x + \mu_y \beta_y + \mu_z \beta_z}{\mu_g} \quad (2)$$

where μ_i and β_i are the components of the μ and β vectors, and μ_g is the ground state dipole moment of a molecule. The axial component of β is given by $\beta_x = \beta_{xxx} + \frac{1}{3} \sum_{j \neq x} (\beta_{xjj} + \beta_{jxj} + \beta_{jxj})$. Another frequently used quantity of interest is the total intrinsic first hyperpolarizability denoted by β_{total} .

$$\beta_{\text{total}} = \sqrt{(\beta_x^2 + \beta_y^2 + \beta_z^2)} \quad (3)$$

The orientationally averaged second hyperpolarizability ($\langle \gamma \rangle$) which is one of the major component of γ obtained from the DFWM measurements has the following expression,

$$\langle \gamma \rangle = \frac{1}{5} [\gamma_{xxxx} + \gamma_{yyyy} + \gamma_{zzzz} + 2(\gamma_{xxyy} + \gamma_{xxzz} + \gamma_{yyzz})] \quad (4)$$

According to Prasad et al. [27], the reorientation contribution to the third-order nonlinearity measured by DFWM experiments is given by Eq. (5) and the quantity within the bracket is known as the polarizability anisotropy ($\Delta\alpha$). For larger anisotropic molecules the reorientation contribution [27] is much smaller than the electronic contribution $\langle \gamma \rangle$.

$$\begin{aligned} \gamma_{\text{or}}^{\text{DFWM}} &= \frac{1}{135kT} [(\alpha_{xx} - \alpha_{yy})^2 + (\alpha_{xx} - \alpha_{zz})^2 + (\alpha_{yy} - \alpha_{zz})^2] \\ &= \frac{2}{135kT} (\Delta\alpha)^2 \end{aligned} \quad (5)$$

where

$$\Delta\alpha = \left\{ \frac{1}{2} [(\alpha_{xx} - \alpha_{yy})^2 + (\alpha_{xx} - \alpha_{zz})^2 + (\alpha_{yy} - \alpha_{zz})^2] \right\}^{1/2}.$$

2.2 The various useful relationships between polarizability and hyperpolarizabilities in the framework of the SOS expressions [20, 21]

The SOS expressions of NLO properties are found to be useful while interpreting their origin with regard to the molecular electronic structure. Moreover, the nonlinear electric response properties arise from the two-photon and

three-photon absorptions besides the linear (one-photon) absorption. The energy of a molecule in presence of a static homogeneous electric field can be expanded as follows

$$\begin{aligned} E(F) &= E^0 - \sum_i \mu_i F_i - \frac{1}{2} \sum_i \sum_j \alpha_{ij} F_i F_j \\ &\quad - \frac{1}{6} \sum_i \sum_j \sum_k \beta_{ijk} F_i F_j F_k \\ &\quad - \frac{1}{24} \sum_i \sum_j \sum_k \sum_l \gamma_{ijkl} F_i F_j F_k F_l \end{aligned} \quad (6)$$

where each of the indices i, j, k, l refers to x, y and z , respectively. The electric field perturbed energy of a molecule can also be expressed as a sum of successive higher energy correction terms.

$$E(F) = E^{(0)} + E^{(1)} + E^{(2)} + E^{(3)} + E^{(4)} + \dots \quad (7)$$

The Kleinman symmetry [33] of indices has been considered in our subsequent derivation. The SOS expression of α_{xy} (Eq. 8) can be obtained from the second-order energy correction $E^{(2)}$ with the Unsold assumption [34] of mean transition energy, ΔE (see Eqs. 22, 23) replacing each resonance energy and using the perturbation operator, $\hat{V} = -\hat{\mu}_x F_x - \hat{\mu}_y F_y - \hat{\mu}_z F_z$ (arising from the interaction between the molecular dipole moment and the incident electric field) in the matrix element $\langle \psi_g | \hat{V} | \psi_n \rangle$, and subsequently on comparing the terms with “ $F_x F_y$ ” in Eqs. 6 and 7.

$$\alpha_{xy} = \frac{2}{\Delta E} \sum_{n \neq g} (\mu_x)_{gn} (\mu_y)_{ng} \quad (8)$$

The term $(\mu_x)_{gn}$ refers to the x -component of transition dipole moment associated with the ground (g) to excited state (n) transition. Likewise, the expression of the nonaxial component of first hyperpolarizability (β_{xyz}) can be found from the third-order energy correction term $E^{(3)}$ and following the above procedure but now comparing the terms with “ $F_x F_y^2$ ” of Eqs. (6) and (7).

$$\begin{aligned} E^{(3)} &= \sum_{n \neq g} \sum_{m \neq g} \frac{V_{gn} V_{nm} V_{mg}}{(E_g^{(0)} - E_n^{(0)}) (E_g^{(0)} - E_m^{(0)})} \\ &\quad - V_{gg} \sum_{n \neq g} \frac{V_{gn} V_{ng}}{(E_g^{(0)} - E_n^{(0)})^2} \\ E^{(3)} &= \frac{F_x F_y^2}{\Delta E^2} \left[\mu_x \sum_{n \neq g} (\mu_y)_{gn} (\mu_y)_{ng} + \mu_y \sum_{n \neq g} \left((\mu_x)_{gn} (\mu_y)_{ng} \right. \right. \\ &\quad \left. \left. + (\mu_y)_{gn} (\mu_x)_{ng} \right) - \sum_{n \neq g} \sum_{m \neq g} \left((\mu_x)_{gn} (\mu_y)_{nm} (\mu_y)_{mg} \right. \right. \\ &\quad \left. \left. + (\mu_y)_{gn} (\mu_x)_{nm} (\mu_y)_{mg} + (\mu_y)_{gn} (\mu_y)_{nm} (\mu_x)_{mg} \right) \right] \end{aligned} \quad (9)$$

$$\begin{aligned} \beta_{xyy} = & \frac{2}{\Delta E^2} \left[\sum_{n \neq g} \sum_{m \neq g} \left((\mu_x)_{gn} (\mu_y)_{nm} (\mu_y)_{mg} \right. \right. \\ & + (\mu_y)_{gn} (\mu_x)_{nm} (\mu_y)_{mg} + (\mu_y)_{gn} (\mu_y)_{nm} (\mu_x)_{mg} \left. \left. \right) \right. \\ & - \mu_x \sum_{n \neq g} (\mu_y)_{gn} (\mu_y)_{ng} - \mu_y \sum_{n \neq g} \left((\mu_x)_{gn} (\mu_y)_{ng} + (\mu_y)_{gn} (\mu_x)_{ng} \right) \left. \right] \end{aligned} \quad (10)$$

The terms in each summation of Eq. 10 can be simplified (see Appendix A) to get the following expressions.

$$\beta_{xyy} = (k' - 1) \frac{\mu_x \alpha_{yy}}{\Delta E} + 2(k - 1) \frac{\mu_y \alpha_{xy}}{\Delta E} \quad (11)$$

$$\beta_x = A \mu_x (3\alpha_{xx} + \alpha_{yy} + \alpha_{zz}) = A \mu_x (2\alpha_{xx} + 3\bar{\alpha}) \quad (12)$$

where $\bar{\alpha}$ is the mean polarizability (Eq. 1).

$$\mu_g \beta_{\text{vec}} \approx \left(1 - \frac{1}{k}\right) \frac{15}{2} \bar{\alpha}^2 = C \bar{\alpha}^2 \quad (13)$$

$$\beta_{\text{vec}} = K \frac{\bar{\alpha} \mu_g}{\Delta E} \quad (14)$$

The nonaxial component of second hyperpolarizability (γ_{xxyy}) can be found from the explicit fourth-order energy term $E^{(4)}$ and on comparing the coefficient of term bearing “ $F_x^2 F_y^2$ ” in Eqs. 6 and 7.

$$\begin{aligned} \gamma_{xxyy} = & \frac{4}{\Delta E^3} \left[\sum_{m \neq g} \sum_{n \neq g} \sum_{p \neq g} \left((\mu_x)_{gm} (\mu_x)_{mn} (\mu_y)_{np} (\mu_y)_{pg} \right. \right. \\ & + (\mu_x)_{gm} (\mu_y)_{mn} (\mu_x)_{np} (\mu_y)_{pg} + (\mu_y)_{gm} (\mu_x)_{mn} (\mu_y)_{np} (\mu_x)_{pg} \\ & + (\mu_y)_{gm} (\mu_y)_{mn} (\mu_x)_{np} (\mu_x)_{pg} + (\mu_x)_{gm} \\ & \times (\mu_y)_{mn} (\mu_y)_{np} (\mu_x)_{pg} + (\mu_y)_{gm} (\mu_x)_{mn} (\mu_x)_{np} (\mu_y)_{pg} \\ & + \sum_{m \neq g} \left\{ \mu_x^2 (\mu_y)_{gm} (\mu_y)_{mg} + \mu_y^2 (\mu_x)_{gm} (\mu_x)_{mg} \right. \\ & + 2\mu_x \mu_y (\mu_x)_{gm} (\mu_y)_{mg} + 2\mu_x \mu_y (\mu_y)_{gm} (\mu_x)_{mg} \left. \right\} \\ & - 2 \sum_{m \neq g} \sum_{n \neq g} \left\{ \mu_x (\mu_x)_{gm} (\mu_y)_{mn} (\mu_y)_{ng} + \mu_y (\mu_y)_{gm} (\mu_x)_{mn} (\mu_x)_{ng} \right. \\ & + \mu_x (\mu_y)_{gm} (\mu_y)_{mn} (\mu_x)_{ng} \\ & + \mu_y (\mu_x)_{gm} (\mu_x)_{mn} (\mu_y)_{ng} + \mu_y (\mu_x)_{gm} \\ & \times (\mu_y)_{mn} (\mu_x)_{ng} + \mu_x (\mu_y)_{gm} (\mu_x)_{mn} (\mu_y)_{ng} \left. \right\} \\ & - \sum_{m \neq g} \sum_{n \neq g} \left\{ (\mu_x)_{gm} (\mu_x)_{mg} (\mu_y)_{gn} (\mu_y)_{ng} \right. \\ & + (\mu_x)_{gm} (\mu_y)_{mg} (\mu_y)_{gn} (\mu_x)_{ng} + (\mu_x)_{gm} (\mu_y)_{ng} (\mu_x)_{gn} (\mu_y)_{ng} \\ & + (\mu_y)_{gm} (\mu_y)_{mg} (\mu_x)_{gn} (\mu_x)_{ng} + (\mu_y)_{gm} (\mu_x)_{mg} (\mu_x)_{gn} (\mu_y)_{ng} \\ & \left. + (\mu_y)_{gm} (\mu_x)_{mg} (\mu_y)_{gn} (\mu_x)_{ng} \right\} \end{aligned} \quad (15)$$

This expanded SOS expression of γ_{xxyy} can further be simplified (see Appendix B) to get the following relations.

$$\begin{aligned} \gamma_{xxyy} = & -\frac{2}{\Delta E^2} \left(\mu_x^2 \alpha_{yy} + \mu_y^2 \alpha_{xx} \right) - \frac{2}{\Delta E} \alpha_{xx} \alpha_{yy} \\ & - \frac{4}{\Delta E} (\mu_x \beta_{xyy} + \mu_y \beta_{yxx}) \\ = & 2 \left(1 - \frac{1}{k} \right) \frac{\alpha_{xx} \alpha_{yy}}{\Delta E} - \frac{4(k' - 1)}{\Delta E^2} \left(\mu_x^2 \alpha_{yy} + \mu_y^2 \alpha_{xx} \right) \end{aligned} \quad (16)$$

For the highly polar molecules, the dipolar terms should contribute rather dominantly compared to the nondipolar term. Equation 16 can further be simplified by replacing the nonaxial components of β from Eq. 11.

$$\gamma_{xxyy} = 2 \left(1 - \frac{1}{k} \right) \frac{\alpha_{xx} \alpha_{yy}}{\Delta E} - \frac{4(k' - 1)}{\Delta E^2} \left(\mu_x^2 \alpha_{yy} + \mu_y^2 \alpha_{xx} \right) \quad (17)$$

$$\gamma_{xxyy} = 2 \left(1 + \frac{1}{k} - \frac{2k'}{k} \right) \frac{\alpha_{xx} \alpha_{yy}}{\Delta E} = K \frac{\alpha_{xx} \alpha_{yy}}{\Delta E} \quad (18)$$

Equations 17 and 18 are appropriate for both polar and nonpolar molecules. The axial component of third-order polarizability can be written as follows.

$$\begin{aligned} \gamma_{xxxx} = & \frac{4}{\Delta E^2} (2k^2 - 3) \mu_x^2 \alpha_{xx} - \frac{8}{\Delta E} \mu_x \beta_{xxx} + \frac{2}{\Delta E} (k - 3) \alpha_{xx}^2 \\ \gamma_{xxxx} = & 6 \left(k - 1 - \frac{1}{k} \right) \frac{\alpha_{xx}^2}{\Delta E} - \frac{8}{\Delta E} (\mu_x \beta_{xxx}) \\ \approx & 6(k - 1) \frac{\alpha_{xx}^2}{\Delta E} - \frac{8}{\Delta E} (\mu_x \beta_{xxx}) \end{aligned} \quad (19)$$

It has recently been shown [29] that both terms in Eq. 19 can be made equivalent to each other, and for a number of dipolar indigo derivatives γ_{xxxx} was found to increase linearly with $\mu_x \beta_{xxx}/\Delta E$. Thus, the contribution arising from the second term of Eq. 19 should be taken as positive. Now Eq. 4 can be written as

$$\langle \gamma \rangle \approx k'' \frac{\bar{\alpha}^2}{\Delta E} \quad (20)$$

Using Eq. 13, $\langle \gamma \rangle$ can also be expressed alternatively as

$$\langle \gamma \rangle \approx k_1'' \frac{\mu_g \beta_{\text{vec}}}{\Delta E} \quad (21)$$

Equation 20 may be used for both polar and nonpolar molecules while Eq. 21 is appropriate only for dipolar molecules.

Since our main concern is the molecular hyperpolarizabilities the mean transition energy, ΔE in the above equations has been calculated as before [29] from the following equation

$$\Delta E = \sqrt{\frac{N_e}{\alpha_{xx}}} \quad (22)$$

where N_e is the total number of electrons of a molecule and α_{xx} is the x -component of polarizability tensor.

Sylvain and Csizmadia [35] obtained an expression of mean transition energy in terms of the occupied molecular orbital energy (ϵ_i) and the number of doubly occupied MOs (N) by optimizing suitable scaling parameters with respect to minimization of the difference between the calculated and experimental mean polarizability ($\bar{\alpha}$) tensor for a number of molecules.

$$\frac{1}{\Delta E} = \frac{1}{N} \sum_i^N -\frac{1}{\epsilon_i} \quad (23)$$

However, ΔE of a molecule calculated from Eq. 22 with linear polarizability calculated at MP2/6-31+G*//B3LYP/6-31+G* level closely agrees with that calculated from Eq. 23 with its B3LYP/6-31+G* calculated occupied orbital energies as can be seen for some representative molecules **1b**, **1g** and **1i** (Scheme 1) for which the mean transition energy values are 19.29 versus 18.35 eV, 17.61 versus 17.17 eV and 17.39 versus 16.96 eV, respectively.

Here, it should be noted that the relative contribution of higher lying excited electronic states to the hyperpolarizabilities decreases with increase in the energy gap from the ground state. This follows from the definition of the oscillator strength (f_{mg}) of a molecule.

$$f_{mg} = \frac{2m_e}{3e^2\hbar^2} \Delta E_{mg} |\mu_{mg}|^2 \quad (24)$$

In this equation, ΔE_{mg} refers to the energy gap between the excited ($|m\rangle$) and the ground ($|g\rangle$) states, μ_{mg} is the corresponding transition moment integral, m_e and e are the mass and charge of electron, respectively. Since for the electronic transition the maximum value of f_{mg} is 1, the increase of energy gap should lower the transition moment according to Eq. 24. Since the SOS expressions of hyperpolarizabilities (Eqs. 10, 15) contain terms with the transition energies in the denominator and the transition moments in the numerator it is expected that the higher energy excited states should have a rather smaller contributions to them.

3 Results and discussion

3.1 NLO properties of representative monomers of Scheme 1

The SCF and MP2 calculated ground state total dipole moment (μ_g), mean polarizability ($\bar{\alpha}$), second-order polarizability (β_{vec}), and third-order polarizability ($\langle\gamma\rangle$) of some monomers **1d_m**, **1d'_m**; **1e_m**, **1e'_m** and **1n_m**, **1n'_m** corresponding to the spirodimers **1d**, **1d'**; **1e**, **1e'** and **1n**, **1n'** in Scheme 1 obtained at the B3LYP/6-31+G* optimized geometry have been presented in Table 1. It can be seen that replacement of tetrahedral carbon by silicon atom lowers the dipole moment for molecules **1d'** versus **1d** and **1e'** versus **1e**. However, Si substitution increases dipole moment in the case of DA substituted molecule (**1n'** vs. **1n**). This specific trend is found at both the HF and MP2 level. It is interesting to note that although the effect of Si substitution is relatively small it increases $\bar{\alpha}$ of the chosen monomers. As expected from Eq. 14, the molecules **1n** versus **1n'** having larger μ_g and $\bar{\alpha}$ but smaller ΔE (Table 2) possess much larger β values. The relative variation of β_{vec} at the MP2 level including the effect of Si substitution can be rationalized using Eq. 14. The electron correlation (EC) effect appreciably increases the β_{vec} (by more than three times) in the case of DA substituted compounds. The inclusion of EC also enhances $\langle\gamma\rangle$ by about three times. The variation of the average second hyperpolarizability among the monomers follows the variation of $\bar{\alpha}$ (Eq. 20). The invariably larger value of $\langle\gamma\rangle$ associated with Si can also be accounted for the larger $\bar{\alpha}$ value.

3.2 Component wise third-order polarizability of representative monomers of Scheme 1

The MP2 calculated mean transition energy (ΔE), axial components of linear polarizability, axial and nonaxial components of third-order polarizability of the chosen

Table 1 The HF/6-31+G*//B3LYP/6-31+G* and MP2/6-31+G*//B3LYP/6-31+G* calculated ground state dipole moment (μ_g , D) and static linear ($\bar{\alpha}$, 10^{-23} esu) and nonlinear (β_{vec} and β_{tot} , 10^{-30} and $\langle\gamma\rangle$, 10^{-36} esu) optical parameters of some monomers of spirodimers in Scheme 1

Molecule ^a	HF				MP2				
	μ_g	$\bar{\alpha}$	β_{vec}	$\langle\gamma\rangle$	μ_g	$\bar{\alpha}$	β_{tot}	β_{vec}	$\langle\gamma\rangle$
1d_m	5.355	3.504	15.30	72.4	4.764	3.248	32.97	32.97	226.5
1d'_m	3.472	3.781	17.32	91.8	3.365	3.447	25.60	25.60	277.6
1e_m	3.838	3.315	15.08	67.7	2.737	3.075	20.04	18.37	191.4
1e'_m	2.981	3.530	12.69	72.9	2.028	3.250	17.88	16.87	198.5
1n_m	10.70	3.468	45.82	81.2	8.046	3.498	165.29	162.96	280.6
1n'_m	11.87	3.732	56.18	105.7	9.017	3.707	186.21	183.39	351.2

^a The subscript 'm' used to denote the monomer to the corresponding spirodimer

Table 2 The MP2/6-31+G*//B3LYP/6-31+G* calculated transition energy (ΔE , eV), axial component of static linear polarizability (α , 10^{-23} esu) and second hyper-polarizability (γ , 10^{-36} esu) of some monomers of spirodimers in Scheme 1

Molecule ^a	ΔE	α_{xx}	α_{yy}	α_{zz}	γ_{xxxx}	γ_{yyyy}	γ_{xxyy}	γ_{zzzz}
1d_m	14.37	5.633	2.852	1.259	754.6	60.2	137.3	10.0
1d'_m	14.09	6.294	2.637	1.409	1045.7	41.5	116.6	20.0
1e_m	14.58	5.471	2.551	1.204	693.8	36.2	98.9	8.9
1e'_m	14.48	5.968	2.420	1.362	806.93	23.2	69.0	10.6
1n_m	13.79	6.229	2.984	1.280	1021.4	73.3	138.9	11.8
1n'_m	13.54	6.937	2.757	1.428	1467.2	40.0	118.5	6.4

^a The subscript ‘m’ used to denote the monomer to the corresponding spirodimer

monomers have been reported in Table 2. For a given molecule, the magnitude of the axial component γ_{xxxx} depends on α_{xx} (ΔE being constant) (see Eq. 18 for $x = y$). The highest value of γ_{xxxx} is obtained for the dipolar molecule **1n'**. For each molecule γ_{xxyy} value lies in between γ_{xxxx} and γ_{yyyy} such that $\gamma_{yyyy} < \gamma_{xxyy} \ll \gamma_{xxxx}$. This order follows from Eq. 18 for the variation $(\alpha_{yy})^2 < (\alpha_{xx}, \alpha_{yy}) \ll (\alpha_{xx})^2$. The replacement of tetrahedral carbon atom by silicon atom increases γ_{xxxx} and γ_{zzzz} but decreases γ_{yyyy} , which have also been reflected by the corresponding components of α . However, γ_{xxyy} invariably decreases on silicon substitution.

3.3 Effect of electron correlation on the NLO properties of spiroconjugated molecules in Scheme 1

At the B3LYP/6-31+G* optimized geometry the HF and MP2 calculated ground state dipole moment (μ_g), mean polarizability ($\bar{\alpha}$), second-order polarizability (β_{vec}) and third-order polarizability ($\langle \gamma \rangle$) for molecules of Scheme 1 have been reported in Table 3. Excepting a few (**1c**, **1e** and **1e'**) the remaining molecules in the first set (**1a–1f'**) are nonpolar and have $\beta = 0$. The molecules of the second set are the DA substituted spiomolecules. The incorporation of EC, in general, lowers the ground state dipole moment. The electron correlation however, has a different effect, on the mean polarizability ($\bar{\alpha}$). For molecules **1a–1f'** and **1n–1o'** which are structurally very much similar with respect to the π -conjugation $\bar{\alpha}$ decreases in most cases due to EC. On the other hand $\bar{\alpha}$ increases for the DA spirocompounds (**1g–1m'**) possessing similar kind of π -conjugation. Thus following the variation of the ground state dipole moment and mean polarizability, the extent of electron correlation effect on β_{vec} of dipolar compounds can be understood from Eq. 13. The EC, in general, enhances β_{vec} of the latter by more than two times. This kind of enhancement of β is fairly consistent with that obtained for a typical DA

π -conjugative molecule p-nitroaniline (PNA) [36]. The similar effect of EC on β at the MP2 level was also noted for larger dipolar molecules [37, 38]. However, the decrease of β_{vec} of **1e** arising from EC may be considered as an exception although such an instance is also known [39]. For the dipolar compounds **1n** and **1n'** β_{vec} (MP2 vs. HF) increases by an order of magnitude (more than a factor of 3.5). It should be noted that inclusion of electron correlation enhances $\langle \gamma \rangle$, in general, by about three times. The increase of $\langle \gamma \rangle$ of dipolar species can be explained by the relative variation of the dominant term ‘ $\mu_g \beta_{vec}$ ’ in Eq. 21. The rather strong enhancement of $\langle \gamma \rangle$ arises from the appreciable increase of β_{vec} . The good linear correlation (MP2 vs. HF) of NLO parameters, $R = 0.98$ for β_{vec} and 0.99 for $\langle \gamma \rangle$ has been noted for the investigated spirocompounds. Hence, a fairly reasonable trend of NLO parameters should be predicted at either level of calculations. This observation is consistent with the recent theoretical investigation [22] of the NLO properties for larger molecules calculated at various levels.

3.4 NLO properties of spirocompounds in scheme 1

Let us first examine the effect of basis set on the calculated NLO properties. For this purpose, we have considered molecule **1h** of Scheme 1 as a representative spiomolecule and calculated the linear and nonlinear optical parameters at the MP2 level for a number of basis sets. The B3LYP/6-31+G* calculated equilibrium geometry has been used in each single point MP2 calculation. It has been noted that inclusion of diffuse function enhances the ground state dipole moment and also the NLO properties although the addition of hydrogen “p-functions” does not have any noticeable effect. The percentage of increase of electric properties can be found on comparing the values calculated without and with diffuse functions (6-31G* vs. 6-31+G*): (6-311G* vs. 6-311+G*): μ_g (6.6/4.8); $\bar{\alpha}$ (13.1/9.0); β_{tot} (11.8/10.2); $\langle \gamma \rangle$ (19.5/19.0). However, the 6-31+G* basis set compared to the 6-311+G** basis set overestimates μ_g , β_{tot} and $\langle \gamma \rangle$ by 2.5, 2.1 and 2.5%, respectively, while it underestimates $\bar{\alpha}$ by 0.78%. Thus, the choice of basis set used in the present investigation seems to be appropriate.

In our subsequent discussion, the MP2 calculated values of the quantities in Table 3 have been considered. It should be noted that the calculated β_{vec} and β_{total} are same for the weakly polar molecules **1b**, **1c**, **1e** and **1e'**. The DA substituted molecules **1g–1h'** and **1n–1o'** have identical values of both β_{vec} and β_{total} while for the remaining molecules β_{total} is significantly larger than β_{vec} . On increasing the polyene chain (molecules **1a–1d**) both the calculated mean linear polarizability and third-order polarizability increase which is consistent with Eq. 20. Let us now compare the effect of spiroconjugation around the

Table 3 The HF/6-31+G*//B3LYP/6-31+G* and MP2/6-31+G*//B3LYP/6-31+G* calculated ground state dipole moment (μ_g , D) and static linear ($\bar{\alpha}$, 10^{-23} esu) and nonlinear (β_{vec} and β_{tot} , 10^{-30} and $\langle \gamma \rangle$, 10^{-36} esu) optical parameters of Scheme 1 molecules

Molecule	HF				MP2				
	μ_g	$\bar{\alpha}$	β_{vec}	$\langle \gamma \rangle$	μ_g	$\bar{\alpha}$	β_{tot}	β_{vec}	$\langle \gamma \rangle$
1a	0.004	1.503	0.00	5.2	0.003	1.549	0.10	0.00	14.0
1b	0.655	2.549	3.63	14.1	0.697	2.497	5.66	5.44	61.8
1c	1.712	3.699	3.57	34.7	1.586	3.564	7.98	7.98	92.6
1d	0.002	6.477	0.00	119.8	0.001	5.961	0.03	0.00	362.9
1d'	0.002	6.851	0.00	142.5	0.001	6.211	0.02	0.00	413.8
1e	3.871	6.157	13.82	111.6	2.501	5.700	8.69	8.69	328.7
1e'	3.764	6.421	10.31	113.8	2.481	5.890	15.97	15.97	325.6
1f	0.002	6.145	0.00	110.5	0.002	5.548	0.06	0.00	376.0
1f'	0.002	6.313	0.00	100.6	0.002	5.703	0.02	0.00	324.5
DA^a									
1g	14.66	4.800	78.51	156.2	12.11	5.193	109.63	109.63	410.0
1g'	15.53	5.188	92.49	184.3	12.69	5.683	231.57	231.57	505.2
1h	18.33	8.729	259.46	889.6	14.52	9.03	631.02	631.02	2510.3
1h'	19.29	9.309	304.08	1051.7	15.09	9.706	762.15	762.15	3415.7
1i	15.79	7.532	202.83	609.5	12.40	8.097	466.04	452.48	1623.8
1i'	15.88	8.091	231.57	721.3	12.37	8.719	542.74	533.10	1968.4
1j	14.63	7.256	191.90	567.7	12.45	7.749	418.50	381.68	1439.6
1j'	15.47	7.872	228.07	683.4	13.06	8.427	505.83	467.94	1768.9
1k	14.56	7.343	185.87	524.2	11.14	8.031	437.62	417.64	1398.1
1k'	15.53	7.967	222.66	611.3	11.84	8.817	533.50	518.10	1691.3
1l	14.84	6.968	178.99	531.7	13.58	7.367	339.06	323.36	1193.1
1l'	15.59	7.597	220.50	643.9	14.11	8.061	423.41	409.19	1458.6
1m	15.31	7.125	175.57	423.1	12.00	8.014	389.76	376.69	1051.6
1m'	16.51	7.741	211.02	471.9	12.95	8.838	482.38	473.99	1205.7
1n	14.39	6.436	59.56	144.5	11.21	6.523	216.62	216.51	522.4
1n'	15.03	6.758	61.78	115.5	11.48	6.729	222.51	222.17	582.5
1o	11.99	6.049	26.76	35.5	10.58	5.889	60.10	59.87	322.4
1o'	10.09	6.415	29.23	41.6	9.02	6.164	51.10	50.76	354.7

^a Donor–acceptor substituted molecules

tetrahedral C and Si atom, respectively (**1d** vs. **1d'**, **1e** vs. **1e'** and **1f** vs. **1f'**). The molecule **1d'** having spirosilicon possesses larger $\bar{\alpha}$ and hence the larger $\langle \gamma \rangle$ compared to that of **1d**. The molecule **1e'** possesses larger β_{vec} but the same $\langle \gamma \rangle$ value as that of **1e**. However, for molecule **1f'** having the silicon-spirocenter $\langle \gamma \rangle$ decreases. The incorporation of N atom in the ring (**1d** vs. **1e** and **1d'** vs. **1e'**) causes a lowering of $\bar{\alpha}$ which in turn also lowers $\langle \gamma \rangle$. With increasing N atom in the ring (**1d** < **1e** < **1f** and **1d'** < **1e'** < **1f'**) both $\bar{\alpha}$ and $\langle \gamma \rangle$ decrease in the same order especially with silicon spirocenter.

The dipolar molecules (**1g**–**1o'**) possess significant value of the ground state dipole moment and β_{vec} . On increase the polyene chain length (**1h** vs. **1g** and **1h'** vs. **1g'**) all the tabulated quantities increase appreciably. $\langle \gamma \rangle$ increases by an order of magnitude. The variation of β_{vec} follows Eq. 14

while the variation of $\langle \gamma \rangle$ follows Eqs. 20 and 21. It should be noted that apart from the chain length, the pattern of conjugation around the spirocenter also accounts for a notable variation in the NLO responses. Thus increasing the number of conjugated carbon atoms at each side of the spirocenter from 8 (**1g**, **1g'**) through 10 (**1n**, **1n'**) to 12 (**1h**, **1h'**), the ground state polarity as indicated by μ_g becomes the lowest in **1n** and **1n'** and the highest in **1h** and **1h'**. The variation of their calculated NLO parameters can be satisfactorily rationalized from Eqs. 14, 20 and 21.

The compounds **1i** and **1i'** containing five-member hydrocarbon rings each having tetrahedral carbon and attached to the central spiroconjugated ring although have the same conjugation length as that of **1h** and **1h'**, both μ_g and $\bar{\alpha}$ decrease. This causes a substantial reduction of the NLO properties as expected from Eqs. 14 and 21. It should

Table 4 The MP2/6-31+G*//B3LYP/6-31+G* calculated transition energy (ΔE , eV), axial component of static linear polarizability (α , 10^{-23} esu) and second hyper-polarizability (γ , 10^{-36} esu) of Scheme 1 molecules

Molecule	ΔE	α_{xx}	α_{yy}	α_{zz}	γ_{xxxx}	γ_{yyyy}	γ_{xxyy}	γ_{zzzz}
1a	24.32	1.669	1.489	1.489	18.1	1.2	11.3	5.9
1b	19.29	3.478	2.249	1.763	139.3	17.1	35.9	11.1
1c	19.81	4.082	3.941	2.668	135.4	85.8	92.2	10.7
1d	18.32	6.602	6.602	4.679	355.2	355.5	345.0	59.6
1d'	18.08	7.048	7.048	4.539	426.4	427.2	426.0	53.8
1e	18.60	6.406	6.439	4.255	330.6	335.9	318.2	47.4
1e'	18.46	6.761	6.739	4.171	352.1	350.2	335.9	37.8
1f	18.69	6.344	6.344	3.955	402.7	403.0	377.1	43.4
1f'	18.69	6.593	6.592	3.925	358.6	358.8	346.4	37.5
DA^a								
1g	17.61	6.299	5.788	3.490	548.1	472.9	486.4	21.4
1g'	17.43	6.717	6.198	4.135	638.9	577.2	574.4	31.1
1h	14.80	11.714	10.783	4.593	3416.4	2865.1	3080.3	32.4
1h'	14.71	12.164	11.394	5.561	4017.3	3529.6	3698.0	47.5
1i	17.39	9.355	9.365	5.571	3252.6	2957.0	820.9	30.2
1i'	16.81	10.325	9.871	5.963	3550.1	3083.4	1492.1	18.8
1j	18.50	8.525	9.275	5.448	2698.9	3287.0	452.8	41.3
1j'	17.92	9.361	10.11	5.811	3545.4	4353.9	329.6	38.1
1k	17.57	9.457	9.156	5.480	2230.0	2704.3	914.4	24.6
1k'	16.70	10.78	9.820	5.850	2281.4	2316.8	1819.1	23.6
1l	18.85	8.458	8.393	5.249	2185.1	2159.4	703.7	26.6
1l'	18.07	9.473	9.103	5.607	3493.2	3182.3	247.0	17.0
1m	17.75	9.538	9.127	5.377	1834.0	1493.8	910.7	11.5
1m'	16.90	10.826	9.973	5.714	1608.1	1394.0	1439.3	15.0
1n	17.54	7.346	7.244	4.980	628.8	486.5	512.5	95.5
1n'	17.28	7.859	7.577	4.752	726.6	559.8	598.6	70.2
1o	18.03	6.954	6.094	4.621	693.3	412.4	16.4	71.3
1o'	17.88	7.346	6.593	4.553	908.4	432.5	14.5	54.3

^a Donor–acceptor substituted molecules

be noted that the gradual replacement of the five member hydrocarbon rings in the spiromolecules, **1i** and **1i'** with hetero-cycle rings such as pyrrole and thiazole (**1j**–**1m'**) shows irregular changes in μ_g , $\bar{\alpha}$ and ΔE (Table 4) which, however, can account for the relatively smaller β_{vec} (see Eq. 14) of the latter compounds. The appreciable lowering of β_{vec} of molecules **1j**–**1m'** (vs. **1i** and **1i'**) has also been reflected in the significant reduction of their $\langle\gamma\rangle$ value (Eqs. 20, 21). The change in the position of *N* atom in the thiazole ring causes a significant modulation of the higher-order response properties. The presence of nitrogen atom in the thiazole ring at *meta* (vs. *ortho*) position to the acceptor group (NO_2) (**1k**, **1k'** vs. **1j**, **1j'**; **1m**, **1m'** vs. **1l**, **1l'**) lowers the value of μ_g but enhances $\bar{\alpha}$ which as expected from Eq. 13 leads to the notable increase of β_{vec} . In contrast $\langle\gamma\rangle$ decreases significantly which may partly be accounted for the substantial decrease of μ_g (Eq. 21). The similar effect of *N* atom of the thiazole ring on the NLO properties was also noted in our earlier investigation on quinonoid molecular system [28].

The placing of two donor groups in one half and two acceptors in the other half of the spirocenter (**1o** vs. **1n** and **1o'** vs. **1n'**) leads to a significant lowering of both μ_g and $\bar{\alpha}$. This results rather large decrease of β_{vec} (nearly one-fourth) and $\langle\gamma\rangle$ (nearly three-fifth). It can be found that for the DA spirocompounds (Scheme 1) the replacement of spiro-Si with spiro-C does not significantly change μ_g but appreciably enhances $\bar{\alpha}$. This leads to appreciable increase of first hyperpolarizability (Eq. 13) as well as the second hyperpolarizability (Eqs. 20, 21). The difference in the spiroconjugative interaction arising from the Si and C spirocenters has been reflected by the difference in the valence interaction which predicts substantial positive charge (decrease of charge density) on spiro-Si atom in contrast to the negative charge (increase of charge density) on spiro-C atom as obtained from the Mulliken Population Analysis. The origin of increase of $\bar{\alpha}$ and NLO properties of Si spirocompounds compared to C spirocompounds can be understood from the larger value of the transition dipole moments [ground to excited state (μ_{gn}) and excited state to

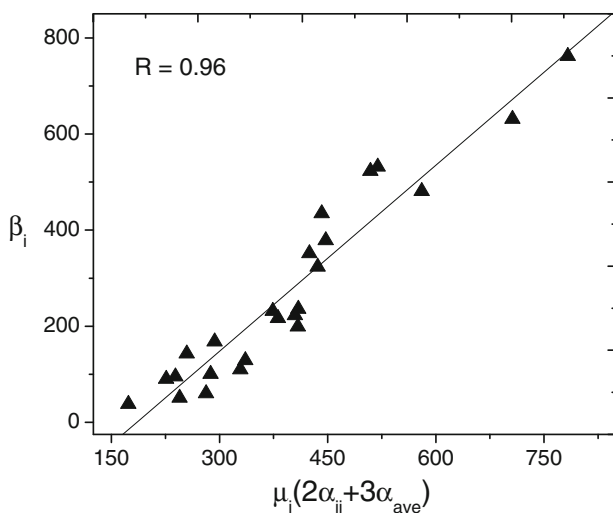


Fig. 1 The plot of β_i versus μ_i ($2\alpha_{ii} + 3\bar{\alpha}$) (Eq. 12) for the DA substituted spirocompounds in Scheme 1. Here, i stands for x , y and z , respectively. The MP2 calculated values of the quantities are used in this and other subsequent plots. α_{ave} in the plots is same as $\bar{\alpha}$

excited state (μ_{mn}) of the formers [16]. This in conjunction with the relatively smaller mean transition energy (ΔE) of Si compounds (Table 4) accounts for their larger values of linear polarizability (Eq. 8) and hyperpolarizabilities (Eqs. 10, 15).

The good linear correlation between the vector-component of quadratic polarizability and the corresponding ground state dipole moment and linear polarizability for the DA spirocompounds (Scheme 1) as expected from Eq. 12 is noted in the plot β_i versus $\mu_i(2\alpha_{ii} + 3\bar{\alpha})$ ($i = x, y, z$) in Fig. 1. The pattern of variation of $\mu_g \beta_{vec}$ with $\bar{\alpha}$ and β_{vec} with $\mu_g \bar{\alpha}/\Delta E$ for the dipolar spirocompounds can be seen in the plots of Fig. 2a, b, respectively, which are fairly consistent with Eqs. 13 and 14. A general qualitative trend between $\langle \gamma \rangle$ and $\bar{\alpha}^2/\Delta E$ (Fig. 3a) for the chosen spirocompounds including both the polar and nonpolar ones conforms Eq. 20. The experimentally measured [27] mean second hyperpolarizability ($\langle \gamma \rangle$) and linear polarizability ($\bar{\alpha}$) of a number of aryl and vinyl derivatives of ferrocene when plotted according to Eq. 20 a fairly good linear correlation ($R = 0.95$) was noted. The plot in Fig. 3b shows that for the chosen spiomolecules the polarizability anisotropy ($\Delta\alpha$) increases linearly with $\bar{\alpha}$. This indicates that for such molecular systems γ_{or}^{DFWM} in Eq. 5 increases with increase in the electronic contribution $\langle \gamma \rangle$ (Eq. 20). This trend has also been noted in earlier theoretical investigation [25]. The calculated $\langle \gamma \rangle$ of the dipolar spirocompounds also bears a nice correlation with $\mu_g \beta_{vec}/\Delta E$ (Fig. 4). The largest value of second- and third-order polarizability has been predicted for the Si spirochromophore **1h'** bearing the DA substituted polyene chain.

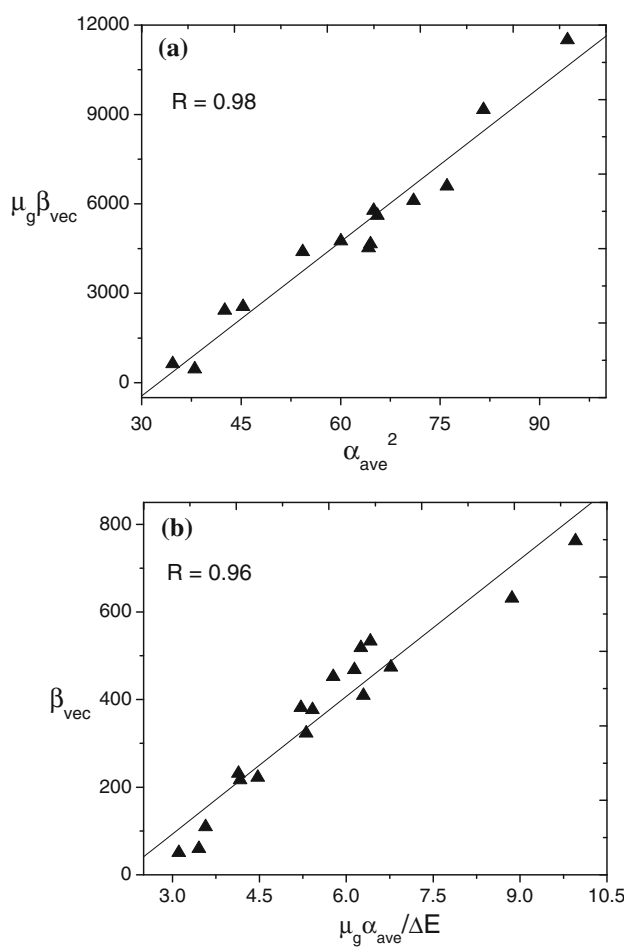


Fig. 2 The plot of **a** $\mu_g \beta_{vec}$ versus $\bar{\alpha}^2$ (Eq. 13) and **b** β_{vec} versus $\mu_g \bar{\alpha}/\Delta E$ (Eq. 14) for the DA substituted spirocompounds in Scheme 1

3.5 Component wise third-order polarizability of spirocompounds in Scheme 1

The MP2 calculated transition energy (ΔE) and components of linear polarizability and third-order polarizability of the investigated spiomolecules (Scheme 1) have been listed in Table 4. Barring a few (**1k**, **1k'**) the highest value of γ_{iiii} of each molecule is associated with the highest value of α_{ii} . For molecules **1d**–**1f** the closer value of the axial components γ_{xxxx} and γ_{yyyy} may be attributed to the nearly identical value of the polarizability components α_{xx} and α_{yy} , respectively (Eq. 18). It is noted that the replacement of the spirocarbon by spirosilicon (**1d'** vs. **1d** and **1e'** vs. **1e**) leads to significant enhancement of γ_{xxxx} , γ_{yyyy} and γ_{xyxy} components but causes slight lowering of the γ_{zzzz} component. This trend of the components of second hyperpolarizability fairly follows the relative variation of the corresponding α components. However, such Si substitution in the nonpolar molecule **1f** (**1f'**) leads to lowering of the tabulated components of γ which may be attributed to the relatively smaller contribution of the first term (three-photon term)

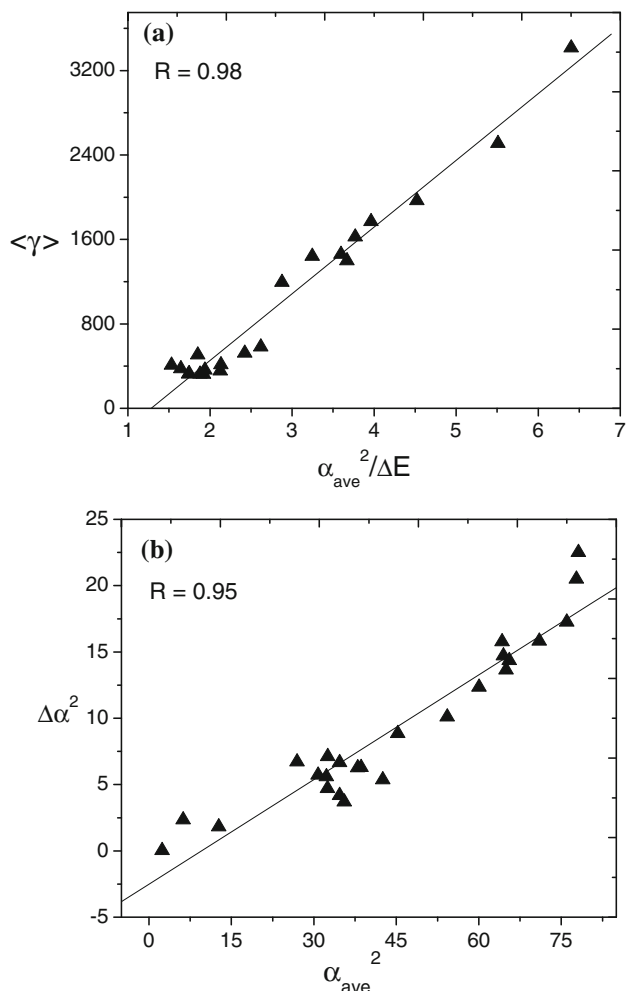


Fig. 3 The plot of **a** $\langle \gamma \rangle$ versus $\bar{\alpha}^2/\Delta E$ (Eq. 20) and **b** $(\Delta\alpha)^2$ versus $\bar{\alpha}^2$ for all spirocompounds in Scheme 1

compared to the fourth term (two-photon term) (Eq. 15) especially for the x - and y -axial components as the dipolar contributions are zero for both molecules.

The replacement of spirocarbon by spirosilicon in general enhances the x - and y -components of γ (with the exceptions, **1k'** vs. **1k** and **1m'** vs. **1m**). For the latter molecules, the exceptional variation of γ_{xxxx} and γ_{yyyy} may arise from the relative contribution of the two terms (α_{xx} and $\mu_x\beta_{xxx}$) in Eq. 19. For the spirocompounds in Scheme 1 the calculated γ_{xxxx} shows a nice linear correlation with $\alpha_{xx}^2/\Delta E$ (Fig. 5). Likewise, γ_{xxyy} (Eq. 18) also bears a good correlation with the square of the geometric mean of α_{xx} and α_{yy} as can be seen in Fig. 6. It should be mentioned that although Eq. 18 can predict a qualitative trend, in general, it is, however, more appropriate for the nondipolar molecules.

It can be seen from Table 4 that for molecules **1i–1m** the value of the nonaxial component γ_{xxyy} is exceptionally smaller (by an order of magnitude) compared to the axial

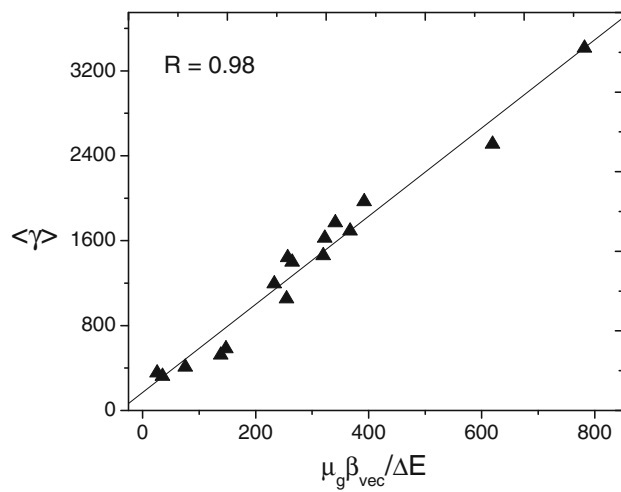


Fig. 4 The plot of $\langle \gamma \rangle$ versus $\mu_g\beta_{vec}/\Delta E$ (Eq. 21) for the donor–acceptor substituted spirocompounds in Scheme 1

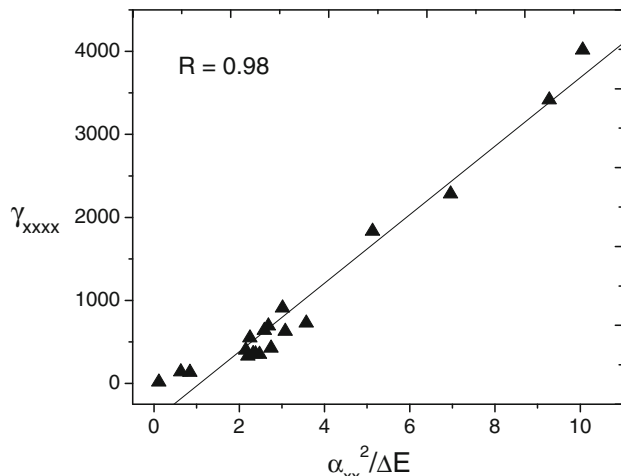


Fig. 5 The plot of γ_{xxxx} versus $\alpha_{xx}^2/\Delta E$ (Eq. 18 for $x = y$) for all spirocompounds in Scheme 1

components. For these molecules, the dipole moment has significant components along both the X - and Y -axis. This makes their nonaxial components β_{xyy} and β_{yxx} (Eq. 11) significant. It should be noted that the product $\mu_x\beta_{xyy}$ and $\mu_y\beta_{yxx}$ for these molecular systems have opposite signs (see Table 5). Therefore, their γ_{xxyy} component as expected from Eq. 16 becomes reasonably smaller due to rather smaller contribution of the second term. The latter term should, however, be appreciable for molecules whose dipole moment lies along a particular axis X or Y (Table 5). This has been shown in the case of dipolar molecules **1e**, **1e'**, **1g–1h'**, **1m'**, **1n** and **1n'** (Table 4) whose nonaxial component γ_{xxyy} does not differ so much from the axial components. However, the rather smaller value of γ_{xxyy} of molecules **1o** and **1o'** compared to the corresponding axial components γ_{xxxx} and γ_{yyyy} can be ascribed to the negligible

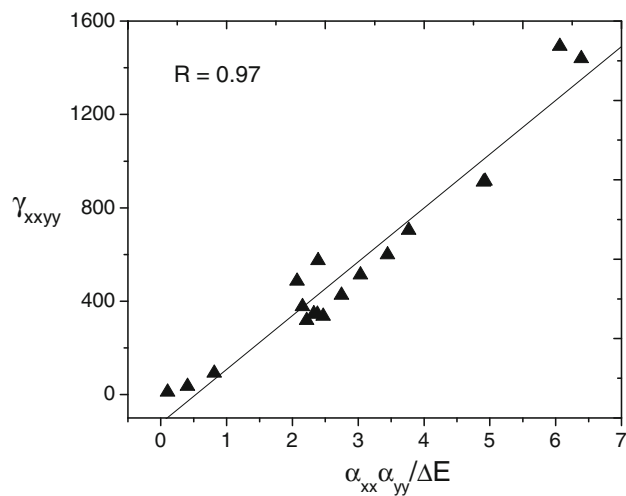


Fig. 6 The plot of γ_{xxyy} versus $\alpha_{xx}\alpha_{yy}/\Delta E$ (Eq. 18) for all spirocompounds in Scheme 1

contribution arising from the dipolar terms (Eqs. 16, 17) as their ground state dipole moment (Table 5) points along the Z-axis.

Let us now examine the change of NLO properties when the monomers form the spirodimers. The monomers **1d_m** and **1d'_m** have significant ground state polarity and first hyperpolarizability which on dimerization through spiro-linkage produce nonpolar centro-symmetric structures and leads to zero first hyperpolarizability. However, their $\langle \gamma \rangle$ increases by about a factor of 1.5 which may arise from the

significant increase of $\bar{\alpha}$. The monomers **1e_m** and **1e'_m** and their corresponding spirodimers possess comparable ground state dipole moment but the calculated β_{vec} of **1e_m** is reduced to almost half while that of **1e'_m** remains almost unchanged in the dimer. The decrease of β_{vec} in the dimer of **1e_m** may arise from the exceptional electron correlation effect as noted earlier [39]. The dipolar molecules **1n** and **1n'** on dimerization, however, lead to significant increase in the ground state dipole moment and NLO properties which can be explained properly by means of Eqs. 14, 20 and 21. It should be noted that although the calculated $\langle \gamma \rangle$ of the spirodimers is larger than the corresponding monomers the components of γ , however, change differently. The component γ_{xxxx} invariably decreases while the components γ_{yyyy} and γ_{xxyy} increase with an order of magnitude in some cases as a result of dimerization. γ_{zzzz} also increases significantly. The notable increase in the α_{yy} and α_{zz} components with $\alpha_{xx} = \alpha_{yy} > \alpha_{zz}$ occurs in the spirodimers **1d–1f** (Table 4) compared to the corresponding monomers (Table 2). Although γ_{xxxx} decreases the other components of γ increase substantially (Tables 2 vs. 4) leading to an overall increase of $\langle \gamma \rangle$ in the dimer. For each of these spiromolecules, the components of γ bear the relation, $\gamma_{xxxx} = \gamma_{yyyy} = \gamma_{xxyy} \gg \gamma_{zzzz}$ which is fairly consistent with Eq. 18.

For the dipolar spirocompounds, the components of γ of the corresponding monomers **1n_m** and **1n'_m** (Table 2) change similarly as noted for the nonpolar ones. The substantial decrease of γ_{xxxx} and increase of γ_{yyyy} due to

Table 5 The MP2/6-31+G*//B3LYP/6-31+G* calculated dipole moment components (μ_i , D), axial and nonaxial components of first hyperpolarizability (β , 10^{-30} esu) of donor–acceptor substituted spiomolecules of Scheme 1

Molecule	μ_x	μ_y	μ_z	β_{xxx}	β_{yyy}	β_{zzz}	β_{xxy}	β_{yxx}
1g	-0.003	12.11	-0.001	-0.06	88.38	-0.001	0.017	99.01
1g'	-0.016	12.70	0.000	-0.46	107.50	0.006	0.127	116.96
1h	0.001	-14.52	0.001	0.04	-298.30	0.003	0.002	-329.62
1h'	-0.023	-15.09	-0.008	-2.37	-360.40	-0.029	0.863	-386.76
1i	-6.817	10.27	-1.358	-245.20	287.70	1.827	73.970	131.42
1i'	-5.435	11.09	-0.572	-234.80	307.10	3.106	91.110	202.36
1j	-8.336	9.23	0.590	-206.08	304.25	1.811	73.030	77.97
1j'	9.287	9.11	-1.102	276.72	385.42	-3.321	-76.180	64.09
1k	-5.550	-9.65	0.298	-186.87	-269.46	0.560	85.660	-142.39
1k'	-3.611	-11.27	-0.269	-112.22	-265.94	2.233	66.910	-254.34
1l	-7.373	-11.22	-2.055	-163.71	-210.70	-0.915	60.190	-104.10
1l'	9.489	10.02	-2.954	290.81	286.91	-1.313	-55.630	58.80
1m	-5.241	-10.57	-2.159	-151.10	-210.37	0.997	56.870	-159.68
1m'	-1.778	-12.49	-2.887	-24.33	-224.65	1.920	-4.200	-249.52
1n	-0.678	11.19	0.175	3.02	91.66	-0.617	1.307	100.21
1n'	-0.748	11.45	0.193	1.03	96.26	-0.065	2.611	107.16
1o	1.569	-0.003	10.46	-3.05	-0.01	-12.990	-0.695	-0.02
1o'	1.659	0.008	-8.865	-2.91	0.04	-8.200	-0.250	0.04

dimerization of $\mathbf{1n}_m$ and $\mathbf{1n}'_m$ can be properly explained by using Eq. 19. In the monomers $\mathbf{1n}_m$ and $\mathbf{1n}'_m$ the dipole moment lies along the X -axis and the corresponding axial component β_{xxx} (see Eq. 11 for $x = y$) has the highest value 142.1×10^{-30} esu (vs. $\beta_{yyy} = -8.8 \times 10^{-30}$ esu) and 169.0×10^{-30} esu (vs. $\beta_{yyy} = -4.9 \times 10^{-30}$ esu), respectively. This in turn predicts the highest value of γ_{xxxx} (Eq. 19) for these monomers. But in their spirodimers the dipole moment lies along the Y -axis and this explains the substantial increase (Table 5) of both β_{yyy} and γ_{yyyy} (Eq. 19 for $x = y$). The appreciable enhancement of the γ_{xyyy} (Table 5) arises from the notable increase of β_{yxx} and μ_y (Eq. 16).

4 Conclusions

In the present work, a number of useful relationships between polarizabilities of different orders have been deduced in the framework of the standard SOS scheme. The strong enhancement of mean second hyperpolarizability ($\langle\gamma\rangle$) of the spiroconjugated molecules can be ascribed to the rather significant increase of mean polarizability ($\bar{\alpha}$) which may arise from the spiroconjugative interaction between the two spirolinked units. As in the case of simple π -conjugated chromophores, the spiroconjugative effect is stronger in the DA substituted spirocompounds, and this in turn leads to substantially large optical nonlinearity, especially the third-order polarizability. The nature of π -conjugation around the spirocenter also has a significant impact on the magnitude of NLO properties. The larger NLO responses arising from Si spirocenter compared to the C spirocenter may be attributed to the greater value of transition dipole moment and the smaller mean transition energy. The correct qualitative trend of hyperpolarizabilities for the chosen spirocompounds is predicted at HF level and also at MP2 level. For the chosen spirocompounds electron correlation showed a profound effect on the calculated NLO properties.

The present SOS scheme of analysis is expected to be general and can be used to explain the variation of both the axial and nonaxial components of NLO coefficients for wide range of molecular systems such as clusters, polymeric chromophores, TICT molecular systems without knowing the spectroscopic properties. For the DA spiro-species $\langle\gamma\rangle$ bear a nice correlation with $\bar{\alpha}$ and $\mu_g\beta_{vec}$, respectively. The relatively larger second hyperpolarizability of polar spiomolecules compared to that of the nonpolar or weakly polar spiomolecules arises from the greater contribution of the “ $\mu_g\beta_{vec}$ ” term.

Acknowledgments (NP) and (PKN) acknowledge the grant from UGC, Government of India under Special Assistance Program (SAP) for carrying out this research work.

Appendix A

The first three terms of Eq. 10 can be simplified by using the following Eq. [29] obtained from the generalized TK sum rule [30, 31] as follows.

$$\sum_{m \neq g} (\mu_y)_{gm} (\mu_y)_{mn} = k \mu_y (\mu_y)_{gn} \quad (25)$$

The physical significance of the constant “ k ” was explained in our earlier work [29].

$$\begin{aligned} \sum_{n \neq g} \sum_{m \neq g} (\mu_x)_{gn} (\mu_y)_{nm} (\mu_y)_{mg} &\equiv \sum_{n \neq g} \sum_{m \neq g} (\mu_y)_{gn} (\mu_y)_{nm} (\mu_x)_{mg} \\ &= k \mu_y \sum_{n \neq g} (\mu_x)_{gn} (\mu_y)_{ng} = k \mu_y \frac{\Delta E \alpha_{xy}}{2} \text{ (from Eq. 8).} \end{aligned} \quad (26)$$

$$\begin{aligned} \sum_{n \neq g} \sum_{m \neq g} (\mu_y)_{gn} (\mu_x)_{nm} (\mu_y)_{mg} \\ \approx k' \mu_x \sum_{n \neq g} (\mu_y)_{gn} (\mu_y)_{ng} = k' \mu_x \frac{\Delta E \alpha_{yy}}{2} \end{aligned} \quad (27)$$

$$((\mu_x)_{nm} \approx k' \mu_x)$$

Using the above expressions, one gets Eq. 11. This equation has been used to find the vector components of β as follows.

$$\begin{aligned} \beta_x &= \beta_{xxx} + \beta_{xyy} + \beta_{xzz} = 3(k-1) \frac{\mu_x \alpha_{xx}}{\Delta E} + (k'-1) \\ &\quad \times \frac{\mu_x}{\Delta E} (\alpha_{yy} + \alpha_{zz}) + 2(k-1) \frac{(\mu_y \alpha_{xy} + \mu_z \alpha_{xz})}{\Delta E} \end{aligned} \quad (28)$$

Neglecting the nondiagonal α terms and assuming that $\frac{(k'-1)}{\Delta E} \approx \frac{(k-1)}{\Delta E} = A$ (a constant) one can find Eq. 12. This in conjunction with Eq. 2 can be expressed in term of linear polarizability as

$$\begin{aligned} \mu_g \beta_{vec} &= \mu_x \beta_x + \mu_y \beta_y + \mu_z \beta_z \\ \mu_g \beta_{vec} &= 2A \left(\mu_x^2 \alpha_{xx} + \mu_y^2 \alpha_{yy} + \mu_z^2 \alpha_{zz} \right) + 3A \bar{\alpha} \left(\mu_x^2 + \mu_y^2 + \mu_z^2 \right) \end{aligned} \quad (29)$$

$$= \left(1 - \frac{1}{k} \right) \left[\alpha_{xx}^2 + \alpha_{yy}^2 + \alpha_{zz}^2 + \frac{9}{2} \bar{\alpha}^2 \right] \quad (30)$$

where $\mu_x^2 = \Delta E \alpha_{xx}/2k$ (obtained for “ $n = g$ ” in Eq. 25) has been used in Eq. 29. Rewriting Eq. 30 leads to the following

$$\begin{aligned} \mu_g \beta_{vec} &= \left(1 - \frac{1}{k} \right) \left[\frac{27}{2} \bar{\alpha}^2 - 2(\alpha_{xx} \alpha_{yy} + \alpha_{yy} \alpha_{zz} + \alpha_{xx} \alpha_{zz}) \right] \\ &= \left(1 - \frac{1}{k} \right) \left[\frac{15}{2} \bar{\alpha}^2 + \frac{2}{3} (\Delta \alpha)^2 \right] \end{aligned} \quad (31)$$

Since $\bar{\alpha}^2 \gg (\Delta \alpha)^2$, Eq. 31 can be written as in Eq. 13. Equation 29 can also be expressed as

$$\beta_{\text{vec}} = \left(1 - \frac{1}{k}\right) \left[3 \frac{\bar{\alpha}^2}{\mu_g} + \frac{2(\Delta\alpha)^2}{3 \mu_g} + 3A\bar{\alpha}\mu_g \right] \quad (32)$$

Ignoring the second term of Eq. 32 which is being much smaller compared to the other two terms, and using the relation, $\bar{\alpha} = \frac{2k\mu_g^2}{3\Delta E}$ one gets Eq. 14 as follows.

$$\begin{aligned} \beta_{\text{vec}} &= \left(1 - \frac{1}{k}\right) \left[\frac{\bar{\alpha}\mu_g}{\Delta E} (5k - 3) \right] = \frac{(k-1)(5k-3)}{k} \left[\frac{\bar{\alpha}\mu_g}{\Delta E} \right] \\ &= K \frac{\bar{\alpha}\mu_g}{\Delta E}. \end{aligned} \quad (33)$$

Appendix B

Let us now simplify the successive terms of Eq. 15 using the TK sum rule. Out of six hexadecapolar (three-photon) terms the first four are equivalent while the last two terms are also equivalent to each other.

$$\begin{aligned} &\sum_{m \neq g} \sum_{n \neq g} \sum_{p \neq g} (\mu_x)_{gm} (\mu_x)_{mn} (\mu_y)_{np} (\mu_y)_{pg} \\ &\equiv \sum_{m \neq g} \sum_{n \neq g} \sum_{p \neq g} (\mu_y)_{gm} (\mu_y)_{mn} (\mu_x)_{np} (\mu_x)_{pg} \\ &\equiv \sum_{m \neq g} \sum_{n \neq g} \sum_{p \neq g} (\mu_y)_{gm} (\mu_x)_{mn} (\mu_y)_{np} (\mu_x)_{pg} \\ &\equiv \sum_{m \neq g} \sum_{n \neq g} \sum_{p \neq g} (\mu_x)_{gm} (\mu_y)_{mn} (\mu_x)_{np} (\mu_y)_{pg} \\ &\sum_{m \neq g} (\mu_x)_{nm} (\mu_x)_{mp} = k (\mu_x)_{ng} (\mu_x)_{gp} \end{aligned}$$

For $p = g$, $\sum_{m \neq g} (\mu_x)_{gm} (\mu_x)_{mn} = k \mu_x (\mu_x)_{gn}$

Likewise, $\sum_{p \neq g} (\mu_y)_{gp} (\mu_y)_{pn} = k \mu_y (\mu_y)_{gn}$. Hence one can find the following expression for each of the above four terms.

$$\begin{aligned} &\sum_{m \neq g} \sum_{n \neq g} \sum_{p \neq g} (\mu_x)_{gm} (\mu_x)_{mn} (\mu_y)_{np} (\mu_y)_{pg} \\ &= \sum_{n \neq g} \left[\left\{ \sum_{m \neq g} (\mu_x)_{gm} (\mu_x)_{mn} \right\} \left\{ \sum_{p \neq g} (\mu_y)_{np} (\mu_y)_{pg} \right\} \right] \\ &= \sum_{n \neq g} \left(k \mu_x (\mu_x)_{gn} \times k \mu_y (\mu_y)_{gn} \right) = k^2 \mu_x \mu_y \sum_{n \neq g} (\mu_x)_{gn} (\mu_y)_{ng} \\ &= \frac{k^2}{2} \Delta E \mu_x \mu_y \alpha_{xy} \end{aligned} \quad (34)$$

Again, $\sum_{n \neq g} (\mu_x)_{mn} (\mu_x)_{np} = k (\mu_x)_{mg} (\mu_x)_{gp}$ and $\sum_{n \neq g} (\mu_y)_{gm} (\mu_x)_{mn} (\mu_x)_{np} (\mu_y)_{pg} = k (\mu_y)_{gm} (\mu_x)_{mg} (\mu_x)_{gp} (\mu_y)_{pg}$.

Thus, each of the last two hexadecapolar terms is expressed as follows.

$$\begin{aligned} &\sum_{m \neq g} \sum_{n \neq g} \sum_{p \neq g} (\mu_y)_{gm} (\mu_x)_{mn} (\mu_x)_{np} (\mu_y)_{pg} \\ &= k \left(\frac{\alpha_{xy} \Delta E}{2} \right)^2 = \frac{k}{4} (\Delta E)^2 \alpha_{xy}^2 \end{aligned} \quad (35)$$

It can be shown that the first four terms in the third summation of Eq. 15 is equivalent to each other and can be simplified as follows (see Eq. 26).

$$\begin{aligned} &\mu_x \sum_{n \neq g} \sum_{m \neq g} (\mu_x)_{gn} (\mu_y)_{nm} (\mu_y)_{mg} \\ &\equiv \mu_x \sum_{n \neq g} \sum_{m \neq g} (\mu_y)_{gn} (\mu_y)_{nm} (\mu_x)_{mg} \\ &\equiv \mu_y \sum_{n \neq g} \sum_{m \neq g} (\mu_y)_{gn} (\mu_x)_{nm} (\mu_x)_{mg} \\ &\equiv \mu_y \sum_{n \neq g} \sum_{m \neq g} (\mu_x)_{gn} (\mu_x)_{nm} (\mu_y)_{mg} \\ &= k \mu_x \mu_y \sum_{n \neq g} (\mu_x)_{gn} (\mu_y)_{ng} = k \mu_x \mu_y \frac{\Delta E \alpha_{xy}}{2} \end{aligned} \quad (36)$$

The other two terms with “ yxy ” and “ xyx ” cannot be simplified as such and, therefore, are expressed in terms of the nonaxial components of second-order polarizabilities, β_{xyy} and β_{yxz} using Eq. 10 as follows.

$$\begin{aligned} \sum_{n \neq g} \sum_{m \neq g} (\mu_y)_{gn} (\mu_x)_{nm} (\mu_y)_{mg} &= \frac{\Delta E^2}{2} \beta_{xyy} + \Delta E \mu_y \alpha_{xy} (1 - k) \\ &+ \frac{\Delta E}{2} \mu_x \alpha_{yy} \end{aligned} \quad (37)$$

Likewise,

$$\begin{aligned} \sum_{n \neq g} \sum_{m \neq g} (\mu_x)_{gn} (\mu_y)_{nm} (\mu_x)_{mg} &= \frac{\Delta E^2}{2} \beta_{yxz} + \Delta E \mu_x \alpha_{xy} (1 - k) \\ &+ \frac{\Delta E}{2} \mu_y \alpha_{xx} \end{aligned} \quad (38)$$

On substituting the above expressions for the summation terms, Eq. 15 can be written as follows.

$$\begin{aligned} \gamma_{xyy} &= \frac{4}{\Delta E^3} \left[\left\{ 2k^2 (\Delta E) \mu_x \mu_y \alpha_{xy} + \frac{k}{2} (\Delta E)^2 \alpha_{xy}^2 \right\} \right. \\ &+ \left\{ \frac{1}{2} (\Delta E) \mu_x^2 \alpha_{yy} + \frac{1}{2} (\Delta E) \mu_y^2 \alpha_{xx} + 2 (\Delta E) \mu_x \mu_y \alpha_{xy} \right\} \\ &- \left\{ 2k (\Delta E) \mu_x \mu_y \alpha_{xy} + 2k (\Delta E) \mu_x \mu_y \alpha_{xy} + (\Delta E)^2 \mu_x \beta_{xyy} \right. \\ &+ (\Delta E)^2 \mu_y \beta_{yxz} + 4(1-k) (\Delta E) \alpha_{xy} \mu_x \mu_y + (\Delta E) \mu_x^2 \alpha_{yy} \\ &\left. \left. + (\Delta E) \mu_y^2 \alpha_{xx} \right\} - \left\{ \frac{1}{2} (\Delta E)^2 \alpha_{xx} \alpha_{yy} + (\Delta E)^2 \alpha_{xy}^2 \right\} \right] \end{aligned} \quad (39)$$

Equation 39 on rearranging takes the following form.

$$\begin{aligned}\gamma_{xxyy} = & -\frac{2}{\Delta E^2} \left(\mu_x^2 \alpha_{yy} + \mu_y^2 \alpha_{xx} \right) - \frac{2}{\Delta E} \alpha_{xx} \alpha_{yy} \\ & + \frac{8}{\Delta E^2} (k^2 - 1) \mu_x \mu_y \alpha_{xy} + \frac{2}{\Delta E} (k - 2) \alpha_{xy}^2 \\ & - \frac{4}{\Delta E} (\mu_x \beta_{xyy} + \mu_y \beta_{yxx})\end{aligned}\quad (40)$$

Ignoring the nondiagonal components of α which for most of the molecular species are close to zero, Eq. 40 reduces to Eq. 16. Using Eqs. 16 and 21, Eq. 4 can be written as,

$$\langle \gamma \rangle = \frac{6(3k-1)}{5\Delta E} \bar{\alpha}^2 + \frac{(12k-16)}{15\Delta E} (\Delta \alpha)^2 - \frac{8}{5\Delta E} \mu_g \beta_{\text{vec}} \quad (41)$$

Using Eq. 13 in Eq. 41 one gets,

$$\begin{aligned}\langle \gamma \rangle \approx & \frac{6(3k-1)}{5\Delta E} \bar{\alpha}^2 - \frac{8(k-1)3}{\Delta E k^2} \bar{\alpha}^2 + \frac{(12k-16)}{15\Delta E} (\Delta \alpha)^2 \\ \approx & \left(18k + \frac{60}{k} - 66 \right) \frac{\bar{\alpha}^2}{5\Delta E} \text{ for } [(\Delta \alpha)^2 \ll \bar{\alpha}^2]\end{aligned}\quad (42)$$

Equation 42 is same as Eq. 20 for a constant value of k .

References

- Prasad PN, Williams DJ (1991) Introduction to nonlinear optical effects in molecules and polymers. Wiley, New York
- Nalwa HS, Miyata S (eds) (1997) Nonlinear optics of organic molecules and polymers. CRC Press, New York
- Interrante LV, Hampden-Smith MJ (eds) (1998) Chemistry of advanced materials: an overview. Wiley, New York, p 207
- Kanis DR, Ratner MA, Marks TJ (1994) *Chem Rev* 94:195
- Brédas J-L, Adant C, Tackx P, Persoons A (1994) *Chem Rev* 94:243
- Shelton DP, Rice JE (1994) *Chem Rev* 94:3
- Segura JL, Martin NJ (2000) *Mater Chem* 10:2403
- Luo Y, Norman P, Agren H (1999) *Chem Phys Lett* 303:616–620
- Fu W, Feng J-K, Pan G-B (2001) *J Mol Struct Theochem* 545:157–165
- Kim SY, Lee M, Boo BH (1998) *J Chem Phys* 109:2593–2595
- Feng JK, Sun XY, Ren AM, Yu KQ, Sun CC (1999) *J Mol Struct Theochem* 489:247–254
- Yang G, Su Z, Qin C (2006) *J Phys Chem A* 110:4817–4821
- Abe J, Shirai Y, Nemoto N, Nagase Y (1997) *J Phys Chem A* 101:1–4
- maslak P, Chopra A, Moylan CR, Wortmann R, Lebus S, Rheingold AL, Yap GPA (1996) *J Am Chem Soc* 118:1471–1481
- Plaquet A, Guillaume M, Champagne B, Castet F, Ducasse L, Pozzo J-L, Rodriguez V (2008) *Phys Chem Chem Phys* 10:6223–6232
- Yang Z-D, Feng J-K, Ren A-M (2008) *Chem Phys Lett* 461:9–15
- Sun M, Niu B, Zhang J (2008) *J Mol Struct Theochem* 862:85–91
- Meyers F, Marder SR, Pierce BM, Bredas JL (1994) *Am. Chem.Soc* 116:10703–10714
- Tykiewski RR, Gubler U, Martin RE, Diederich F, Bosshard C, Giinter P (1998) *J Phys Chem B* 102:4451–4465
- Orr BJ, Ward JF (1971) *Mol Phys* 20:513
- Bishop DM (1994) *J Chem Phys* 100:6535
- Isborn CM, Leclercq A, Vila FD, Dalton LR, Brédas JL, Eichinger BE, Robinson BH (2007) *J Phys Chem A* 111:1319–1327
- Waite j, Papadopoulos MG (1990) *J Phys Chem* 94:1755
- Sugino T, Kambe N, Sonoda N, Sakaguchi T, Ohta K (1996) *Chem Phys Lett* 251:125–131
- Kamada K, Ueda M, Nagao H, Tawa K, Sugino T, Shmizu Y, Ohta K (2000) *J Phys Chem A* 104:4723–4734
- Qiu Y-Q, Fan H-L, Sun S-L, Liu C-G, Su Z-M (2008) *J Phys Chem A* 112:83–88
- Ghosal S, Samoc M, Prasad PN, Tufariello JJ (1990) *Phys Chem* 94:2847
- Nandi PK, Panja N, Ghanty TK (2008) *J Phys Chem A* 112:4844–4852
- Nandi PK, Panja N, Ghanty TK, Kar T (2009) *J Phys Chem A* 113:2623–2631
- Bethe HA, Salpeter EE (1977) Quantum mechanics of one and two electron atoms. Plenum, New York
- Kuzyk MG (2001) *IEEE J Sel Top Quantum Electron* 7:774
- Schimdt MW et al (1993) *J Comput Chem* 14:1347
- Kleinman DA (1962) *Phys Rev* 126:1977
- Unsöld A (1927) *Z Physik* 43:563
- Sylvain MG, Csizmadia IG (1987) *Chem Phys Lett* 136:575
- Sim F, Chin S, Dupuis M, Rice JE (1993) *J Phys Chem* 97:1158
- Champagne B, Kirtman B (2006) *J Chem Phys* 125:024101
- Zaleśny R, Papadopoulos MG, Bartkowiak W, Kaczmarek A (2008) *J Chem Phys* 129:134310–134314
- Niewodniczański W, Bartkowiak W (2007) *J Mol Model* 13:793–800